Journal of Power Sources 241 (2013) 400–403

Contents lists available at SciVerse ScienceDirect

Journal of Power Sources

journal homepage: www.elsevier.com/locate/jpowsour

Short communication

Gelation or dispersion of $LiFePO_4$ in water-based slurry?

Jyh-Cheng Tsai [a], Feng-Yen Tsai [a,b], Chih-An Tung [a], Han-Wei Hsieh [b], Chia-Chen Li [a,*]

[a] Department of Materials & Mineral Resources Engineering, National Taipei University of Technology, Taipei 10608, Taiwan
[b] R&D Department, Advanced Lithium Electrochemistry Co., Taoyuan 33068, Taiwan

HIGHLIGHTS

- Commercial $LiFePO_4$ powder may disperse or gel in the water-based slurry.
- Poor quality of carbon coverage causes $LiFePO_4$ to exhibit a large quantity of −OH.
- Poor quality of carbon coverage causes $LiFePO_4$ to gel in the water-based slurry.
- Quality of carbon coverage determines the rheology of water-based $LiFePO_4$ slurry.

ARTICLE INFO

Article history:
Received 27 February 2013
Received in revised form
18 March 2013
Accepted 23 April 2013
Available online 29 April 2013

Keywords:
Lithium-ion battery
Lithium iron phosphate
Gelation
Dispersion
Aqueous slurry

ABSTRACT

The gelation of commercial lithium iron phosphate ($LiFePO_4$) in water-based slurry and its corresponding mechanism are studied. When a large portion of the inner $LiFePO_4$ of commercial carbon-coated $LiFePO_4$ is exposed, the powder becomes polar and its surface possesses numerous hydroxyl groups that tend to form a three-dimensional gel-like structure via hydrogen bonding.

1. Introduction

Since lithium iron phosphate ($LiFePO_4$) was reported as a potential cathode-active material for a lithium-ion battery by Good enough and his coworkers in 1997 [1], it has attracted widespread attention and has been extensively studied during the past decade. The advantages of the olivine-structured $LiFePO_4$ include a large theoretical capacity, good cycle-life performance and safety [2–4]. The excellent structural stability of $LiFePO_4$, which results from the strong Fe–P–O bonds, also greatly increases its thermal stability at high temperatures in its fully charged state [5–7]. In addition, the low cost and toxicity of $LiFePO_4$ due to its environmentally compatible constituents make it a promising cathode-active material for large batteries. Nevertheless, $LiFePO_4$ has some disadvantages, such as poor electrical conductivity ($\sim 10^{-9}$ S cm^{-1}) and diffusion of lithium ions (Li^+) in $LiFePO_4$ [8,9]. These issues result in losses in capacity and rate capability and thus hinder the commercial application of $LiFePO_4$. For the improvement of Li^+ diffusion, the use of fine $LiFePO_4$ particles has been proposed [10,11]. The coating of the surface of $LiFePO_4$ with a conductive material is a commonly used approach to enhance its electrical conductivity [12–16]. Among the various possible conductive coating materials, carbon is the most popular because of its high chemical stability. Because of the differences in techniques used for the synthesis of $LiFePO_4$, commercially produced $LiFePO_4$ powders are available with a wide range of carbon contents that typically range from 1 wt % to 5 wt% [17–20].

For the fabrication of electrodes, electrode materials are typically mixed using either a water-based (aqueous) process or a solvent-based (non-aqueous) process [21–24]. For environmental consistency and cost considerations, the aqueous process is gaining favor and has attracted significant interest. However, the aqueous process has a drawback of tending to cause serious agglomeration of most oxides, including $LiFePO_4$; until now, the only efficient

* Corresponding author. Tel.: +886 2 27712171; fax: +886 2 87733742.
E-mail addresses: ccli@ntut.edu.tw, ccli2761@gmail.com (C.-C. Li).

0378-7753/$ – see front matter © 2013 Elsevier B.V. All rights reserved.
http://dx.doi.org/10.1016/j.jpowsour.2013.04.102

approach to prevent powder agglomeration has been the addition of an appropriate dispersant to the system [25,26]. Furthermore, several reports have noted that not all commercial $LiFePO_4$ powders exhibit the same dispersibility in aqueous slurries [22–26]; i.e. even from the same powder supplier, notable differences in the dispersion properties of the aqueous slurries prepared with powders from different production lots may be observed. This variety in the dispersibility of $LiFePO_4$ powder in water is an important issue that has greatly concerned the $LiFePO_4$-related industry. In addition, the uncertain dispersibility of powders may also confuse the end users of the powder and cause them to imprecisely manipulate the powders to obtain unsuitable electrode slurries. As typical commercial $LiFePO_4$ powders, some of which are available as dispersions and some as gels in water, D-LFP (dispersible $LiFePO_4$) and G-LFP (gelled $LiFePO_4$) are two $LiFePO_4$ powders with the same physicochemical properties of crystallinity, a median particle size (d_{50}) of 2.2 μm and an approximate carbon content of 1.07–1.20 wt %; these powders were acquired from the same supplier. When we processed these powders in water by adding the same ingredients, completely distinct flow behaviors of their as-prepared aqueous slurries were observed. Fig. 1 shows that the aqueous slurry prepared from the powder of D-LFP exhibits fluidity, whereas the other slurry from G-LFP resembles a gel more. As opposed to the easily dripped D-LFP slurry (left), the aqueous G-LFP slurry (right) exhibits stagnant behavior of a gelled jelly that lacks fluidity. Understanding the cause for the deviation in the dispersibility of powders is essential, and this issue needs to be clarified because the formation of powder gels will be detrimental to the electrode-manufacturing process, especially to the steps of slurry-sieving and slurry-casting.

2. Experimental

The cathode-active material used in this study included two types of $LiFePO_4$ powders (Advanced Lithium Electrochemistry, Taiwan) with approximate carbon contents of 1.20 wt% and 1.07 wt %, referred to as D-LFP and G-LFP, respectively, which the carbon contents were determined by an elemental analyzer (Elementar VarioEL III-CHNS, Germany). Both powders had a median size (d_{50}) of 2.2 μm, as measured by the light-scattering (LA300, Horiba, Japan) method. Synthetic graphite (Timrex KS6, Timcal A + G Sins, Switzerland) with a d_{90} of 5.8–7.1 μm and carbon black (CB; Super-P, Timcal A + G Sins, Switzerland) with an average size of 40 nm were used as conductive agents. The binder used was styrene butadiene rubber (SBR, Asahi Kasei, Japan) in the form of an aqueous emulsion of 48 wt% with a viscosity of 130 mPa·s at 25 °C. Sodium carboxymethyl cellulose (SCMC, Aldrich, USA) was used as a thickening agent for the SBR with an $\overline{M_n}$ of 250,000 g mol^{-1} and a degree of substitution (DS) of 1.2; the SCMC was mixed with SBR in a ratio of 5:12. Deionized water was used as a solvent in this study.

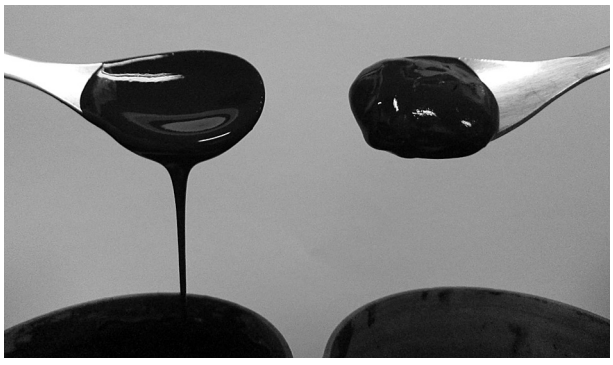

Fig. 1. Pictures of aqueous slurries of D-LFP (left) and G-LFP (right).

The surface chemistries of $LiFePO_4$ powders were characterized by the techniques known as the electroacoustic method (ZetaProbe, Colloidal Dynamics, USA) and the Fourier-transformed infrared (FT-IR) spectroscopy (DA8.3, Bomem, Canada); the FT-IR spectra were obtained in the transmission mode on pressed $LiFePO_4$ pellets mixed with KBr. For the measurements of zeta potentials, aqueous powder suspensions with a solid loading of 5 wt% $LiFePO_4$ were prepared. The pH levels of the powder suspensions were adjusted by the addition of aqueous solutions of hydrochloric acid or sodium hydroxide. For rheological measurements, water-based electrode slurries with 64.1 wt% $LiFePO_4$ powder were prepared by the mixing additives of 2.1 wt% KS6, 4.2 wt% Super-P, 2.6 wt% SBR and 1.1 wt% SCMC. Notably, the solid loading of $LiFePO_4$ was based upon the weight of deionized water, and the contents of all additives were based upon the mass of $LiFePO_4$ powder. The electrode slurries were de-agglomerated and mixed by being ball-milled at 1000 rpm with Y_2O_3-stabilized ZrO_2 media for 1.5 h at room temperature. The rheologies of the electrode slurries were analyzed using a concentric-cylinder rheometer (AR1000, TA Instruments, UK). Cone-plate geometry fixtures of 20 mm diameter and a cone angle of 1° were chosen for the dynamic frequency sweep tests; the dynamic sweeps were performed with an angular frequency (ω) varying from 0.6283 to 628.3 rad s^{-1} at a given strain in the linear viscoelastic regime.

3. Results and discussion

As the result shown in Fig. 1, D-LFP and G-LFP are two $LiFePO_4$ powders received from the same supplier with exhibiting similar physicochemical properties; however, the former is suspended in the aqueous slurry and the latter is gelled. In order to clarify the mechanism that caused different fluidity between the aqueous slurries of D-LFP and G-LFP, we investigated the surface chemistries of these two powders in water. Fig. 2 shows a comparison of the zeta potentials of these two powders in water. Interestingly, these two powders exhibit distinct differences in the variations of their zeta potentials as functions of pH, although their other physicochemical properties are indiscriminate. For D-LFP, the zeta potential is less negative at lower pH levels, and increases with pH. For G-LFP, however, the variation of the zeta potential with pH is

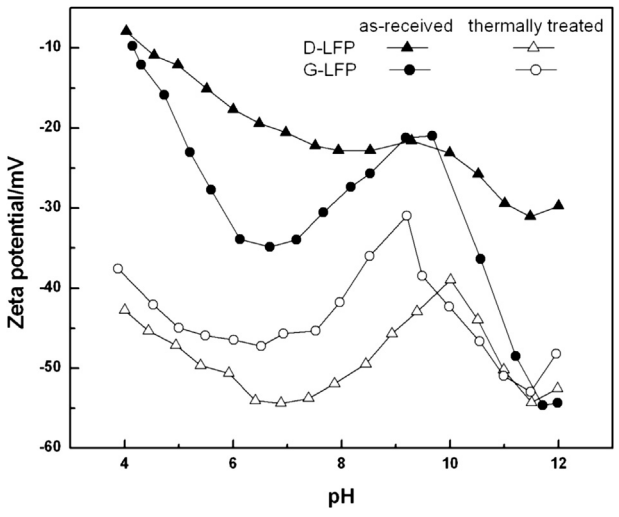

Fig. 2. Zeta potentials as a function of pH for as-received and thermally treated D-LFP and G-LFP.

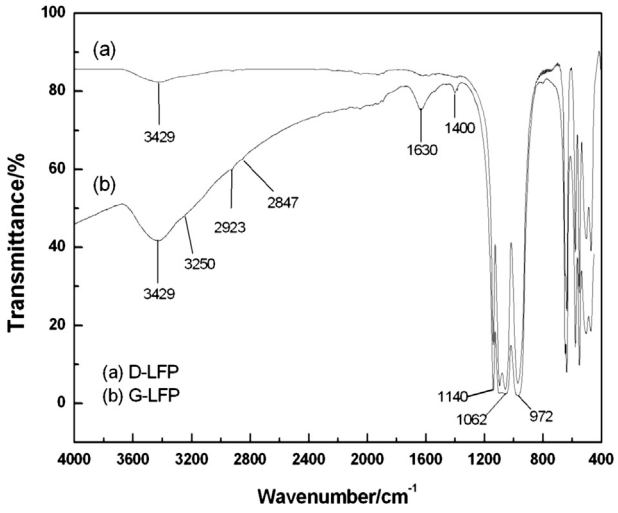

Fig. 3. FT-IR spectra of (a) D-LFP and (b) G-LFP.

complicated. The zeta potential initially increases with pH at pH < 6.5, decreases in the pH range of 6.5–9.5 and then increases again at pH > 9.5. Similar to most oxide materials, $LiFePO_4$ is dissolvable in water. According to the literature [27–30], numerous chemical species are generated after dissolution of $LiFePO_4$, such as Li_3PO_4, LiOH, Li_2HPO_4, $FePO_4$, $Fe(OH)_2$, FeOOH and Fe_2O_3. These species may exist in the aqueous slurry or specifically adsorb onto the surface of $LiFePO_4$. When specific adsorption occurs, the surface composition of the $LiFePO_4$ powder will be complex, and we hypothesize that this complexity is the reason for the abnormal variation of the zeta potential that occurred at pH > 6.5 for G-LFP in Fig. 2. In contrast, the simple variation of zeta potentials with pH for D-LFP suggests that the specific adsorption of the dissolved species onto this powder is unfavorable and that the covering quality of the carbon on the D-LFP is probably different from that on the G-LFP; i.e. D-LFP is more likely to be covered with a strengthened carbon layer or is more likely to be completely covered with carbon. The carbon coating dominates the surface chemistry and makes the surface less polar and unfavorable for the specific adsorptions of the polar species dissolved from $LiFePO_4$. Contrarily, because the zeta potentials of G-LFP are more sensitive to pH and because these zeta-potential values are significantly greater than those of D-LFP, G-LFP must have a polar surface, i.e. the chemical or physical structure of the carbon coverage on G-LFP should be incomplete or full of defects, which must result in a large exposure of inner $LiFePO_4$. When the inner $LiFePO_4$ is significantly exposed, the surface chemistry of G-LFP will be dominated by the polar $LiFePO_4$, which facilitates the specific adsorption of the dissolved species. Furthermore, in order to show the strong effect of the surface carbon coverage on the zeta potentials of carbon-coated $LiFePO_4$, we also measured the zeta potentials of D-LFP and G-LFP that were thermally pre-treated at 420 °C in air for 4 h. The results show that the zeta-potential variations of the thermally treated D-LFP and G-LFP are approximately the same as those of the as-received G-LFP (Fig. 2), which indicates that incomplete coverage of carbon made the powder more polar and caused it to have a more complex surface chemistry.

In addition to our analyses of the zeta potentials, we also performed FT-IR spectroscopic analyses to compare the surface chemistry of D-LFP and G-LFP. For the D-LFP powder shown in Fig. 3(a), the IR features in the spectrum are the strong P–O stretch at 900–1200 cm^{-1} and the weak O–H vibration at 3429 cm^{-1} [30]. The spectrum of the G-LFP powder shown in Fig. 3(b) has the same IR transmittances as those of D-LFP but with much more intense O–H vibration. In addition, other features related to the O–H bending at 1630 cm^{-1} due to the physically adsorbed water, the C–H bending at 1400 cm^{-1} and the C–H stretches at 2923 cm^{-1} and 2847 cm^{-1} were noted. The more significant C–H features at 2923 cm^{-1}, 2847 cm^{-1} and 1400 cm^{-1} suggest that more carbon defects appeared on G-LFP than on D-LFP. Because of the greater number of carbon defects, a greater amount of the inner polar $LiFePO_4$ exposed to the particle surface of G-LFP can be anticipated. This greater exposure has been evidenced by the existence of the strong features of the hydroxyl groups (–OH) (3429 cm^{-1}) and the adsorption of water vapor (1630 cm^{-1}), which appear only on a polar substrate. Moreover, the IR spectrum of G-LFP reveals a peak shoulder at 3256 cm^{-1}; this special feature is commonly attributed to the O–H vibrations involving intermolecular hydrogen bonds (H-bonds) [31,32], and this result indicates the formation of H-bonds among the G-LFP particles. On the basis of the results in Figs. 2 and3, the possible gelation mechanism of G-LFP powder is schemed in Fig. 4. Because the surface coverage of carbon on G-LFP is incomplete and thereby a large amount of the inner $LiFePO_4$ is exposed, the particles can possibly contact each other via the H-bonding of surface–OH to form a three-dimensional (3D) powder-connected (gel-like) structure. Notably, powder gelation must be distinguished from powder agglomeration. In the case of gelation, powder arranges to form a continuous phase, and the liquid is the discontinuous phase that fills the 3D structure. In the case of agglomeration, powder presents as a discontinuous phase that is instead suspended in the continuous liquid.

Fig. 5 compares the viscoelastic properties of the aqueous slurries of D-LFP and G-LFP. These two aqueous slurries exhibit distinct flow behaviors (Fig. 1): one is fluidic and the other is gel-like. These two slurries, however, demonstrate the same results in that they both exhibit an elastic modulus (G') greater than their viscous modulus (G''); these results indicate a more solid-like behavior than a liquid-like behavior for both slurries [33–35]. The solid-like

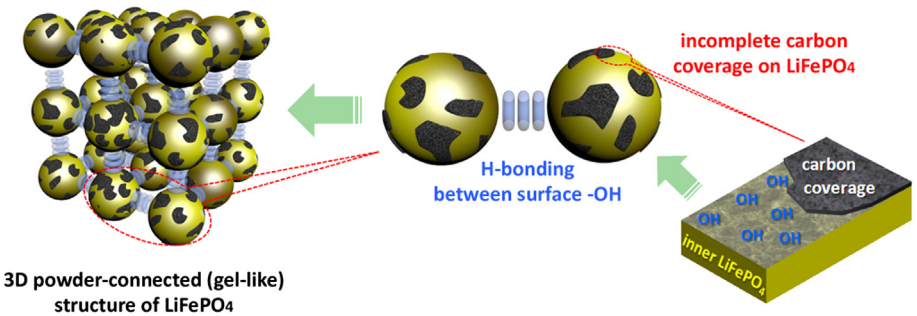

Fig. 4. Possible mechanism for the gelation of G-LFP.

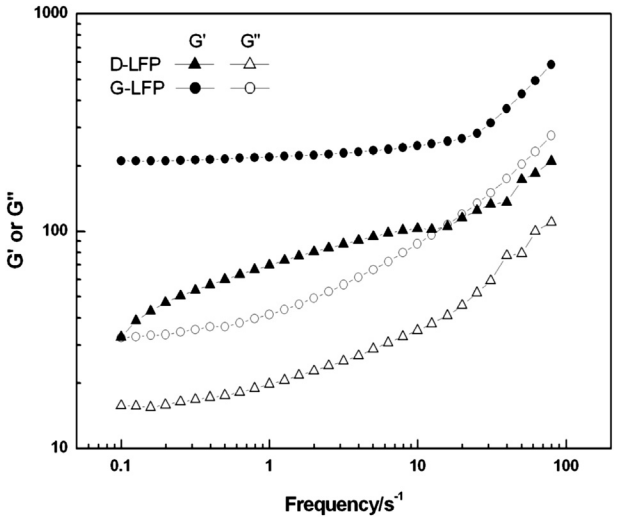

Fig. 5. G' and G'' as functions of sweeping frequencies for 64.1 wt% aqueous slurries of D-LFP and G-LFP.

behavior of the aqueous slurry of G-LFP is apparent given the result shown in Fig. 1, and, as anticipated, the gelation of G-LFP causes the result of $G' > G''$. Nevertheless, the G' of the aqueous slurry of D-LFP is also greater than its G'', although it appears fluid in Fig. 1. Because the 64.1 wt% solid content (based upon the weight of the solvent) of the aqueous slurry of D-LFP is extremely high, the agglomeration of the powder occurs naturally and cannot be avoided, especially when the powder is not particularly dispersed by any dispersant. Therefore, the result of $G' > G''$ for the D-LFP slurry should be primarily attributed to the non-dispersed agglomerates of D-LFP. Certainly, the G-LFP powder may also agglomerate in the aqueous slurry, which would contribute to the result of $G' > G''$; however, the extremely large value of G' for the G-LFP slurry suggests that the gelation of powder is more likely the dominant effect. In addition, the G' of the G-LFP slurry is less dependent on the sweeping frequency than that of the D-LFP slurry, which demonstrates that the G-LFP slurry is more elastic than the D-LFP slurry. This higher elasticity of the G-LFP slurry should be relevant to the better elasticity of the 3D gel-like structure that contains numerous voids which fill with liquid. Moreover, the several-fold increases in the G' and G'' of the slurry of G-LFP compared to the slurry of D-LFP suggests that the particle–particle interactions and the particle–fluid interactions are both larger for the aqueous slurry of G-LFP.

4. Conclusions

In this investigation, a possible mechanism that causes the large difference in the dispersibility of commercial $LiFePO_4$ powders in water has been proposed. The results of zeta-potential and IR spectroscopy experiments suggest that the quality of the coverage of the surface carbon coating determines whether the gelation or the agglomeration of $LiFePO_4$ predominates. The zeta potential results showed that even $LiFePO_4$ powders with the same chemical composition may have distinctly different qualities of carbon surface coatings and therefore different exposures of the inner $LiFePO_4$, which affect the surface chemistry. The IR results showed that different exposures of $LiFePO_4$ lead to a great discrepancy in the quantity of surface–OH groups. When the surface of the commercial $LiFePO_4$ is dominated by the exposed inner $LiFePO_4$ and exhibits a large quantity of–OH groups, the formation of a 3D gel-like structure of powder through the specific interactions of H-bonding can be anticipated.

Acknowledgments

The authors appreciate financial and material supports from the Advanced Lithium Electrochemistry Co.

References

[1] A.K. Padhi, K.S. Nanjundaswamy, J.B. Goodenough, J. Electrochem. Soc. 144 (1997) 1188.
[2] A. Yamada, S.C. Chung, K. Hinokuma, J. Electrochem. Soc. 148 (2001) A224.
[3] N. Iltchev, Y. Chen, S. Okada, J.I. Yamaki, J. Power Sources 119–121 (2003) 749.
[4] G. Arnold, J. Garche, R. Hemmer, S. Ströbele, C. Vogler, M. Wohlfahrt-Mehrens, J. Power Sources 119–121 (2003) 247.
[5] D.D. MacNeil, Z. Lu, Z. Chen, J.R. Dahn, J. Power Sources 108 (2002) 8.
[6] S. Patoux, G. Rousse, J.B. Leriche, C. Masquelier, Chem. Mater. 15 (2003) 2084.
[7] S.C. Yin, P.S. Strobel, H. Grondey, L.F. Nazar, Chem. Mater. 16 (2004) 1456.
[8] P.P. Prosini, M. Lisi, S. Scaccia, M. Carewska, F. Cardellini, M. Pasquali, J. Electrochem. Soc. 149 (2002) A297.
[9] A.S. Andersson, J.O. Thomas, J. Power Sources 97 (2001) 498.
[10] C. Delacourt, P. Poizot, S. Levasseur, C. Masquelier, Electrochem. Solid-State Lett. 9 (2006) A352.
[11] P.P. Prosini, M. Carewska, S. Scaccia, P. Wisniewski, S. Passerini, M. Pasquali, J. Electrochem. Soc. 149 (2002) A886.
[12] H. Huang, S.C. Yin, L.F. Nazar, Electrochem. Solid-State Lett. 4 (2001) A170.
[13] H. Gabrisch, J.D. Wilcox, M.M. Doeff, Electrochem. Solid-State Lett. 9 (2006) A360.
[14] H.T. Chung, S.K. Jang, H.W. Ryu, K.B. Shim, Solid State Commun. 131 (2004) 549.
[15] P.S. Herle, B. Ellis, N. Coombs, L.F. Nazar, Nat. Mater. 3 (2004) 147.
[16] S.T. Myung, S. Komaba, R. Takagai, N. Kumagai, Y.S. Lee, Chem. Lett. 32 (2003) 566.
[17] S.W. Oh, S.T. Myung, S.M. Oh, K.H. Oh, K. Amine, B. Scrosati, Y.K. Sun, Adv. Mater. 22 (2010) 4842.
[18] Y. Wang, Y. Wang, E. Hosono, K. Wang, H. Zhou, Angew. Chem. Int. Ed. 47 (2008) 7461.
[19] Y.D. Choa, G.T.K. Feya, H.M. Kao, J. Power Sources 189 (2009) 256.
[20] M. Gaberscek, R. Dominko, J. Jamnik, Electrochem. Commun. 9 (2007) 2778.
[21] H.Q. Yang, D.P. Li, S. Han, N. Li, B.X. Lin, J. Power Sources 58 (1995) 221.
[22] W. Porcher, B. Lestriez, S. Jouanneau, D. Guyomard, J. Power Sources 195 (2010) 2835.
[23] S.F. Lux, F. Schappacher, A. Balducci, S. Passerini, M. Winter, J. Electrochem. Soc. 157 (2010) A320.
[24] J.H. Lee, H.H. Kim, D.S. Zang, Y.M. Choi, H. Kim, D.K. Yi, W.M. Sigmund, U. Paik, J. Phys. Chem. C 114 (2010) 4466.
[25] C.C. Li, Y.H. Wang, T.Y. Yang, J. Electrochem. Soc. 158 (2011) A828.
[26] C.C. Li, X.W. Peng, J.T. Lee, F.M. Wang, J. Electrochem. Soc. 157 (2010) A517.
[27] Denis Y.W. Yu, K. Donoue, T. Kadohata, T. Murata, S. Matsuta, S. Fujitani, J. Electrochem. Soc. 155 (2008) A526.
[28] W. Porcher, P. Moreau, B. Lestriez, S. Jouanneau, D. Guyomard, Electrochem. Solid-State Lett. 11 (2008) A4.
[29] K. Zaghib, M. Dontigny, P. Charest, J.F. Labrecque, A. Guerfi, M. Kopec, A. Mauger, F. Gendron, C.M. Julien, J. Power Sources 185 (2008) 698.
[30] S. Mustafa, A. Naeem, S. Murtaza, N. Rehana, H.Y. Samad, J. Colloid Interface Sci. 220 (1999) 63.
[31] S. Ji, T. Jiang, K. Xu, S. Li, Appl. Surf. Sci. 133 (1998) 231.
[32] C.C. Li, C.L. Huang, Colloid Surf. A 353 (2010) 52.
[33] C.C. Li, Y.C. Lee, Y.M. Cheng, J. Am. Ceram. Soc. 93 (2010) 3049.
[34] K.B. Shepard, H. Gevgilili, M. Ocampo, J. Li, F.T. Fisher, D.M. Kalyon, J. Polym. Sci. Pol. Phys. 50 (2012) 1504.
[35] Y.S. Song, J.R. Youn, Carbon 43 (2005) 1378.